Supplementary data

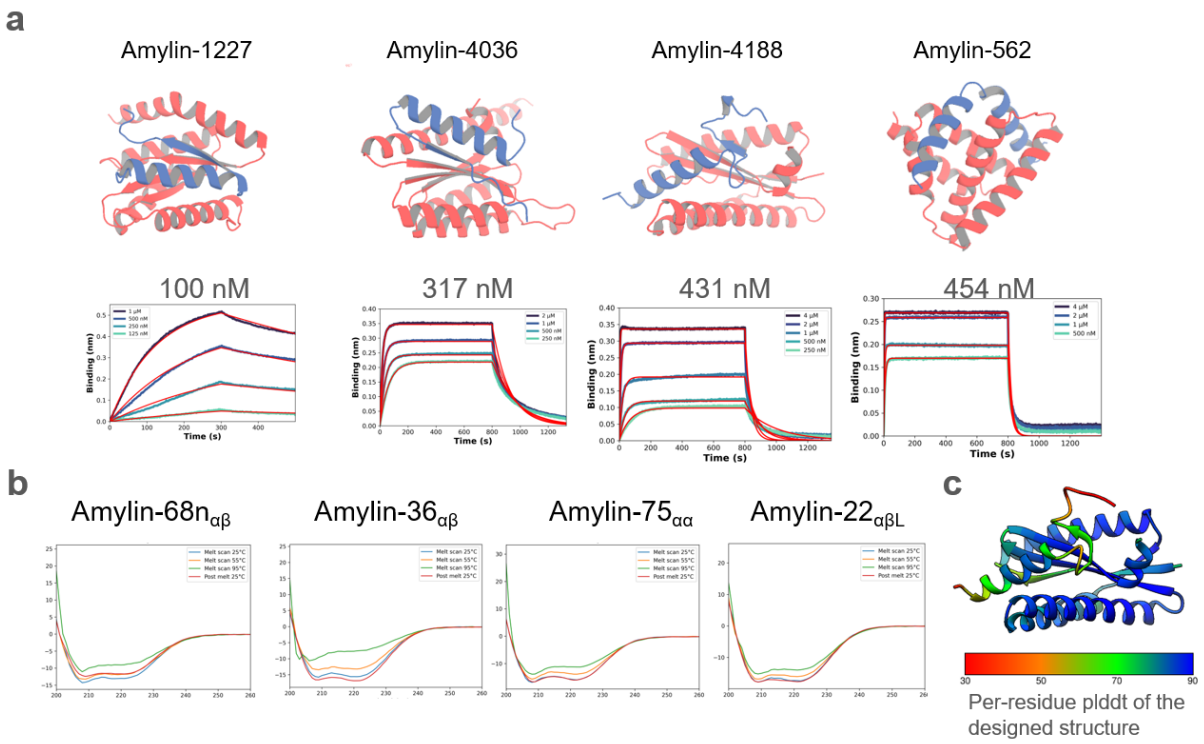

Supplementary figure. 1 Diffusing de novo peptide binder design to Amylin.

a, Top, the designed structures of four initial hits, Amylin-1227, -4036, -4188, -562, which serve as starting point of two sided partial diffusion. Bottom, the BLI result of the four hits revealing the binding affinity of the 4 initial hits are 100, 317, 431, 454 nM, respectively. **b,** Circular dichroism data show that the optimized binders have helical secondary structure and is stable up to 95 °C (inset). **c,** The per residue pLDDT (predicted Local Distance Difference Test) plotting of Amylin-Am22 complex in design.

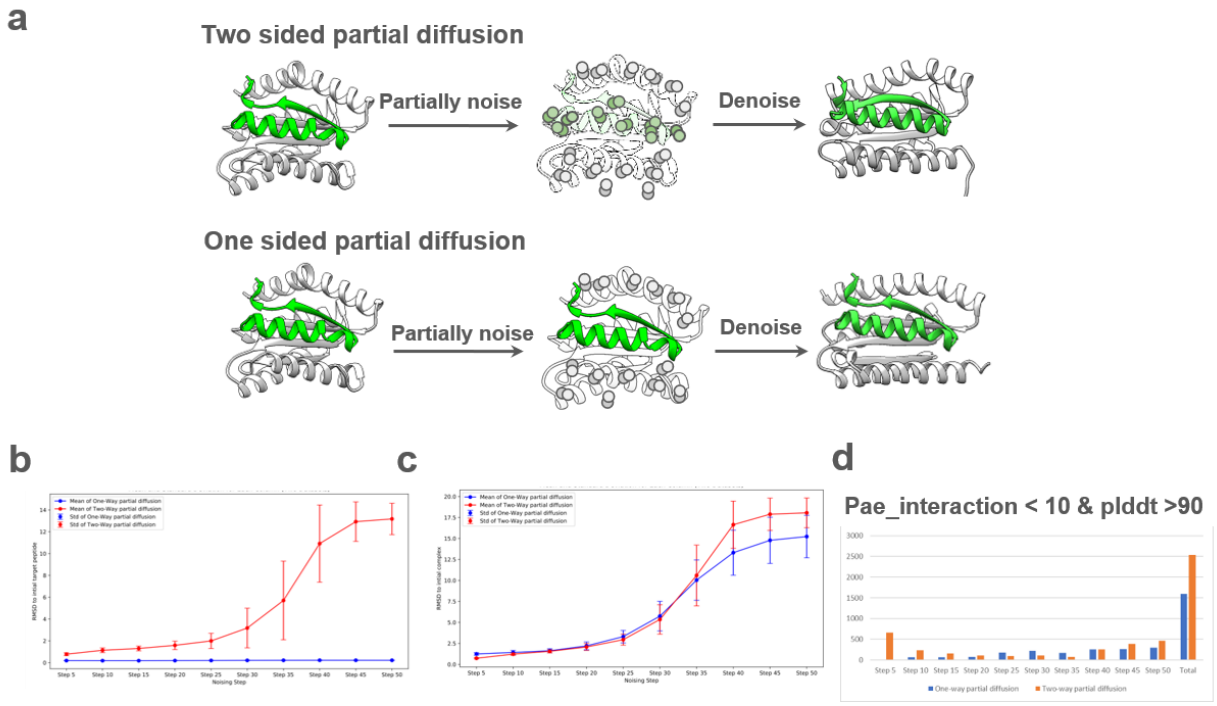

Supplementary figure. 2 Two sided partial diffusion and the comparison with one sided partial diffusion

a, Top, two sided partial diffusion allows simultaneous conformational changes in both the target and the binder. Bottom, one sided partial diffusion solely diversifies the conformation of the binder while keeping the target fixed. **b,** Two sided partial diffusion (in red) diversifies the target while one sided partial diffusion (in blue) keeps the target fixed. **c,** The peptide-binder complex diverse magnitudes of two sided (in red) and one sided partial diffusion (in blue) remain comparable before nosing step 35, after step 35, the diverse magnitude of two sided parietal diffusion is larger than one sided one. **d,** Take the interface pAE <10, pLDDT >90 as cutoff criteron, two sided partial diffusion yielded designs with generally better metrics than one sided diffusion. At steps 25, 30, and 35 exclusively, one-sided partial diffusion exhibited superior performance. However, in practical cases, we typically operate within fewer than 25 steps to remain the main features of parent structure.

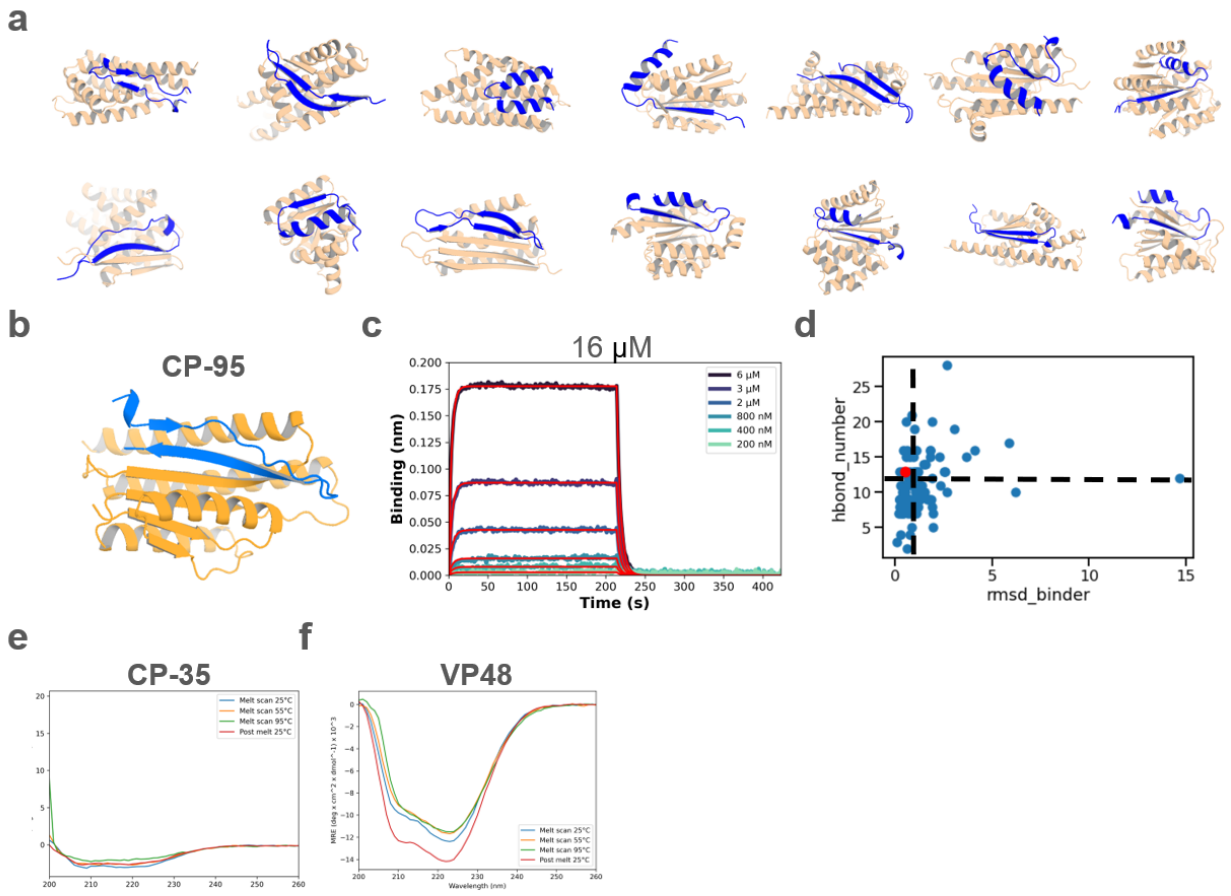

Supplementary figure. 3 Diffusing de novo peptide binder design to C peptide.

a, Sequence-input diffusion was carried out, allowing C peptide to sample diverse conformations. The diverse conformations of C peptide and protein binder are rendered in blue and wheat color, respectively. **b,** Design model of the initial hit CP-95 which was also the starting point of two-sided partial diffusion. **c**, the BLI data revealed the binding affinity of the initial hit is 16 μm. **d,** Scatter plot showing the distribution of designs based on the number of hydrogen bonds (hbond_number) and the RMSD of the binder (rmsd_binder). Each blue dot represents a design, while the red dot marks a validated hit. The dashed black lines indicate the cutoff values based on the initial hit criteria (hbond_number = 13 and rmsd_binder = 0.545). Analysis revealed that only 6 out of 96 designs met these criteria (hbond_number > 13 and rmsd_binder < 0.545), indicating a low success rate. **e-f,** Circular dichroism data show that the binder CP35 (e) and VP48 (f) have helical secondary structure and is stable up to 95 °C (inset).

a

	Trajectories	Helix:Strand:loop	Pae_interaction <10, plddt_binder > 90
Sequence input	10k	5.7:3.8 :0.5	23
Strand specification	10k	0.54:8.9:0.6	1,192

b

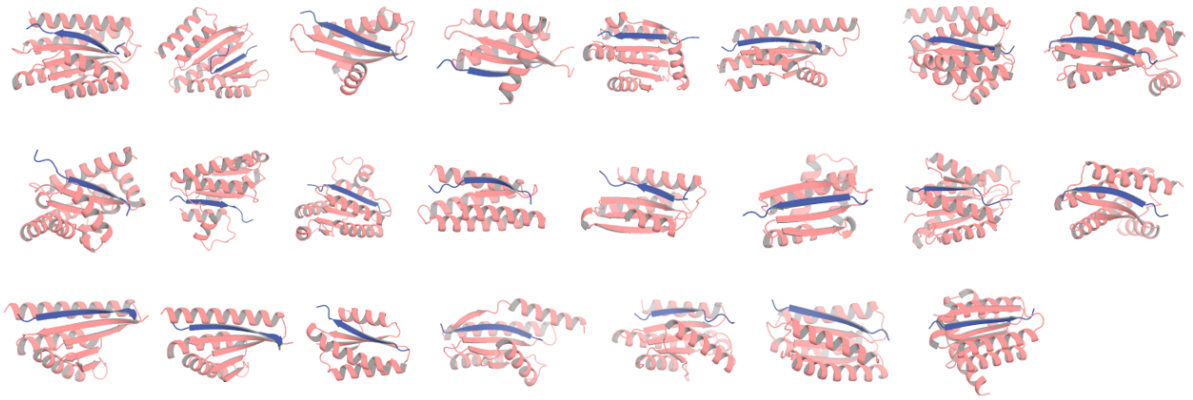

c

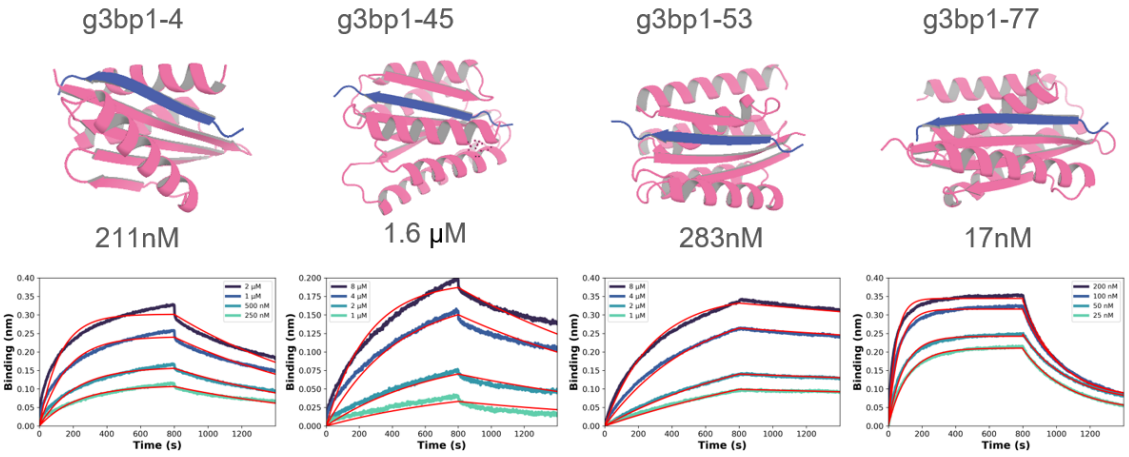

d G3bp1-11

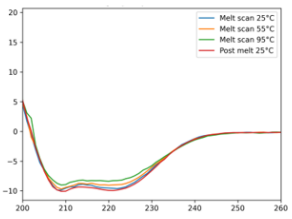

e IL2RG-30

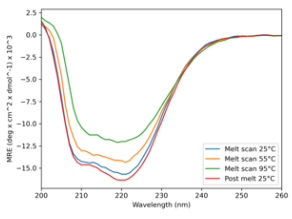

Supplementary figure. 4 Diffusing de novo peptide binder design to G3BP1^{RBD}.

a, Comparative analysis of structural outcomes between sequence input and strand specification approaches in protein design. The table presents the number of trajectories (10k) and the distribution of secondary structures (Helix:Strand: Loop) for both methods. This table counts the successful cases where the Pae_interaction < 10 and the plddt_binder score > 90, noting 23 successes with sequence input and 1,192 with strand specification. This reflects an approximately 51-fold increase in efficacy with the strand specification method, highlighting its superior performance in achieving desired structural configurations. **b**,The 23 successful cases designed using sequence input RFdiffusion all feature targets in strand conformation. **c**, Design models and BLI data of the 4 initial hits of G3BP1^{RBD} which was also the starting point of two sided partial diffusion. **d and e,** Circular dichroism data show that the G3bp1-11 binder (d) and IL2RG-30 binder (e) have helical secondary structure and are stable up to 95 °C (inset).

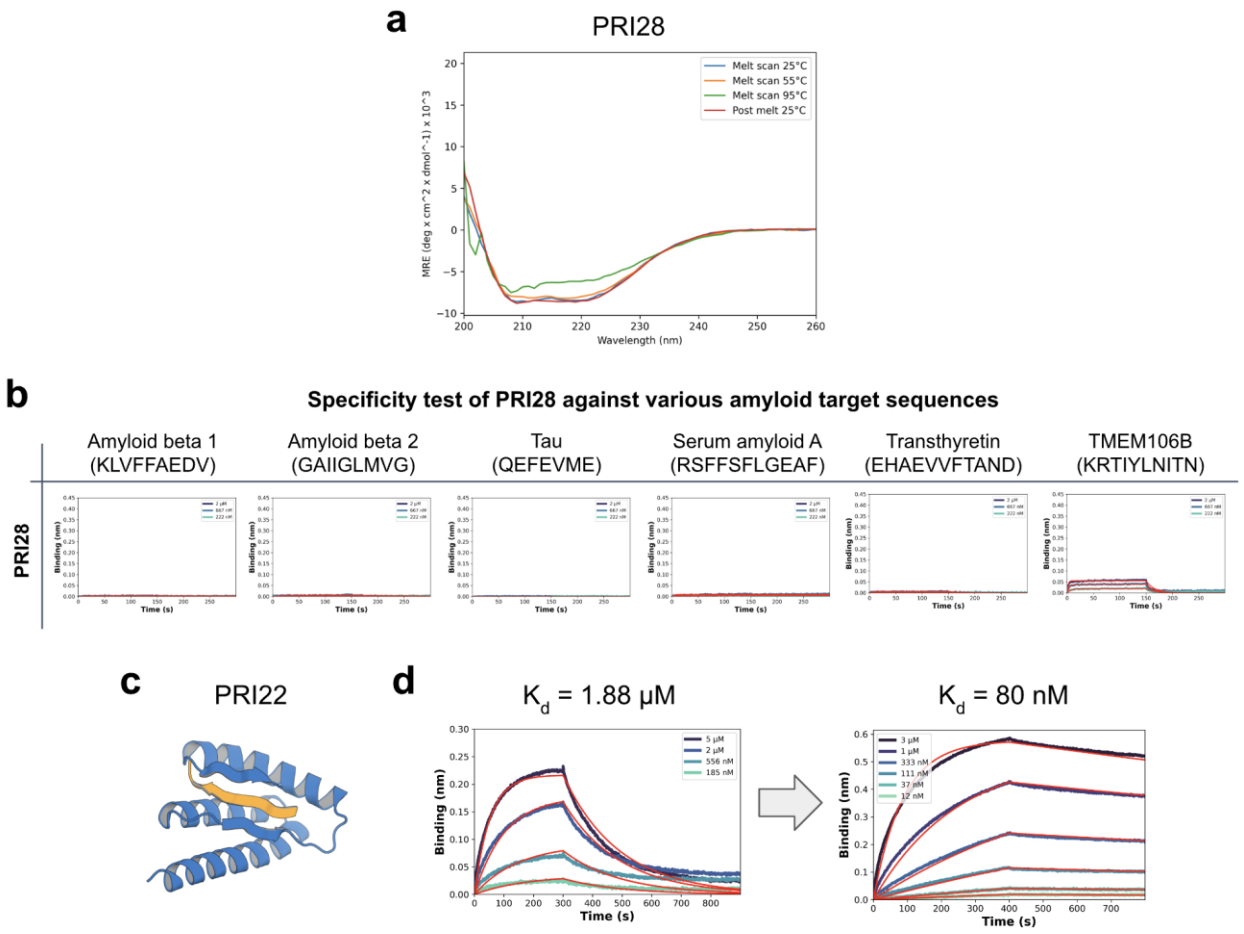

Supplementary figure. 5 Diffusing de novo peptide binder design to prion protein.

a, Circular dichroism data show that the PRI28 binder has helical secondary structure and is stable up to 95 °C. **b**,The specificity test for prion binder PRI28 against various amyloid target sequences showed that PRI28 is highly specific, with some cross-reactivity observed only with TEME106B, related to Fig. 2h. **c,** The design model of PRI22, designed using target sequence information alone, is shown. **d**, The BLI data revealed that the binding affinity of PRI22 is 1.88 µM (left), which improved to 80 nM after two-sided partial diffusion (right).

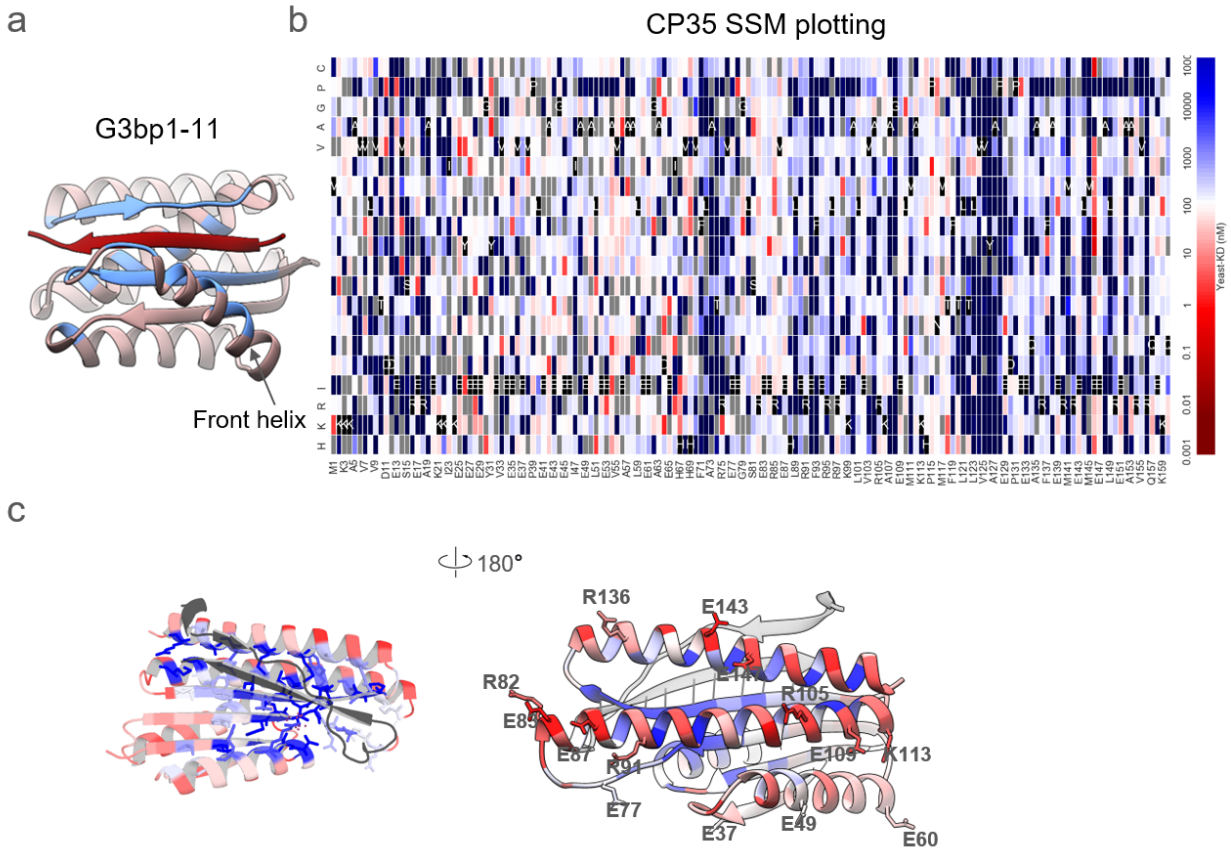

Supplementary figure. 6 SSM analysis of CP35.

a, The crystal structure of G3bp1-11, positioned 4 Å away from the target on the binder, is marked in blue. **b**, Full SSM maps for the design of CP35. **c**, Zoomed-in views of the residues presented in the surface region, as shown in Figure 3e.

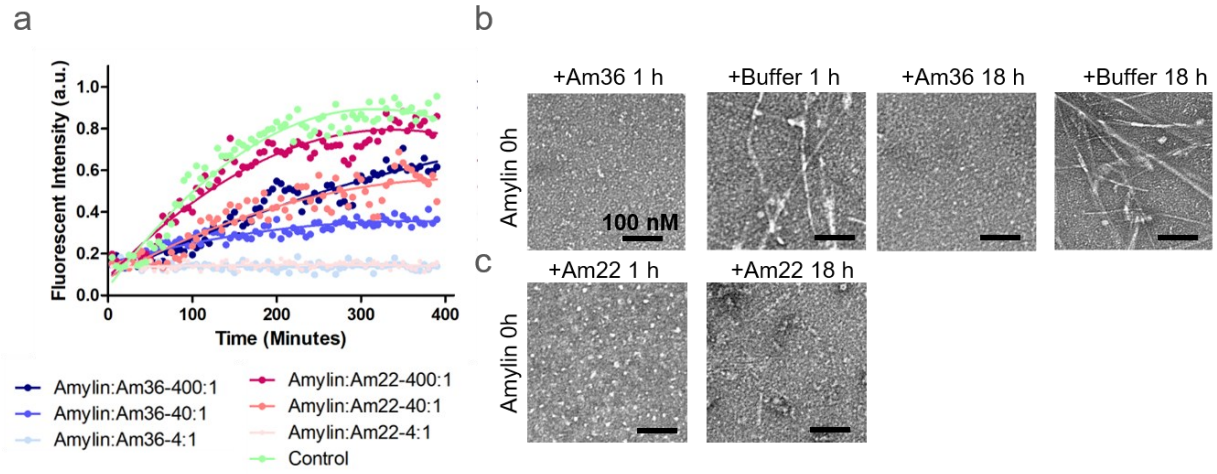

Supplementary figure. 7 Designs inhibit Amylin fibril formation and dissociate existing fibrils

a,Amylin binders Amylin-22$_{\alpha\beta L}$ and Amylin-36$_{\alpha\beta}$ inhibit fibril formation in a concentration-dependent manner. The initial concentration of Amylin monomer was 10 μM, with subsequent additions of binders at 2.5 μM, 0.25 μM, and 0.025 μM, establishing molar ratios of binder to Amylin of 1:4, 1:40, and 1:400, respectively. **b-c** ,, Negative stain electron microscopy images were taken of 40 μM Amylin monomer samples following the addition of 10 μM Amylin-36$_{\alpha\beta}$ (b) and Amylin-22$_{\alpha\beta L}$ (c) at 1 hour and 18 hours, respectively. Scale bars, 100 nM.

IDP name	Targeted Sequence	Position
Amylin	KCNTATCATQRLANFLVHSSNNFG AILSSTNVGSNTY (37)	Full length
C peptide	EAEDLQVGQVELGGGPGAGSLQP LALEGSLQ (31)	Full length
VP48	DALDDFDLDMLGSDALDDFDLDML PADALDDFDLDMLGS (39)	Full length
G3BP1	KPGFGVGRGLAPR (13)	453-465
Common gamma chain	ERLCLVSEIP (10)	327-336
Prion	VNITIKQH (8)	180-187

Supplementary table 1. Summary of IDPs and IDRs in the study, detailing each protein's sequence and positional data within their respective structures.

Supplementary Video Legends

Supplementary Video 1

A video of the sequence input diffusion trajectory for the fully diffused Amylin-binder complex.

Methods

De novo peptide binder design given only sequence input using RFdiffusion and ProteinMPNN

For each target, approximately ten to fifty thousand diffused designs were generated given only sequence input of the target. The resulting library of backbones were sequence designed using ProteinMPNN, followed by AF2+initial guess[23]. The resulting designs were filtered based on interface pAE, pLDDT. In addition, AF2 monomer was performed using only the binder sequence without the peptide to filter based on the monomer pLDDT of the binder and RMSD to the binder design model. Subsequently, FastRelax was executed to obtain Rosetta metrics. The resulting binders were then further filtered based on criteria including contact_molecular_surface, ddG, SAP score and the numbers of hydrogen bonds. Specific filtering criteria were carefully selected to narrow down the set to 48 to 96 designs for each target.

Two sided partial diffusion to optimize binders

Partial diffusion enables the input structure to be noised only up to a user-specified timestep instead of completing the full noising schedule. The starting point of the denoising trajectory is therefore not a random distribution. Rather, it contains information about the input distribution resulting in denoised structures that are structurally similar to the input. Unlike one sided directional partial diffusion, which solely diversifies the conformation of the binder while keeping the target fixed, two sided partial diffusion allows simultaneous conformational changes in both the target and the binder. The input designs were subjected to 15 noising timesteps out of a total of 50 timesteps in the noising schedule, and subsequently denoised. Approximately ten to fifty thousand partially diffused designs were generated for each target. The resulting library of backbones were sequence designed using ProteinMPNN, followed by AF2+initial guess[23]. The resulting designs were filtered in the same way as the designs from the aforementioned sequence input diffusion process.

Integrating secondary structure specifications into RFdiffusion

To permit specification of the secondary structure (but not three-dimensional coordinates) of the peptide target, a modified version of RFdiffusion was trained that permits specification of the secondary structure of a region, along with its sequence. The training strategy largely followed

that used to train previous RFdiffusion models [11,14], with some modifications. A summary is provided below.

Overview of "base" RFdiffusion Training: Rfdiffusion[14] is a denoising diffusion probabilistic model (DDPM), which is fine-tuned from the RoseTTAFold structure prediction model[22,42]. In RFdiffusion, the N-Ca-C frame representation (translation and orientation) of protein backbones[22,43] is used, and, over 200 discrete timesteps, these backbone frames are corrupted following a defined forward noising process that noises these frames to distributions indistinguishable from random distributions (three-dimensional Gaussian distribution for translations, and uniform SO(3) distribution for rotations). RFdiffusion is trained to reverse this noising process, predicting the true (X0) protein structure at each timestep of prediction (starting from randomly sampled translations and rotations). Successive predictions are used to "self-condition" predictions through an inference trajectory, and mean squared error (MSE) losses minimize the error between forward and reverse processes. Full details of training are described in Watson et al[14].

Modifications to permit secondary structure specification of the target: As in the original RFdiffusion fine-tuned for protein binder design, RFdiffusion was trained 50% of the time on single chains from the Protein Data Bank (PDB) < 384 amino acids in length, and 50% on hetero-complexes. In the latter case, one chain (< 250 amino acids in length) was designated the "binder", and when necessary the other "target" chain was radially cropped around the interface (to 384 – the length of the "binder" residues). For single chain examples, 20% of the time, the whole backbone was noised, and in the other 80% of cases 20-100% of the protein backbone was noised. For hetero-complex examples, the whole "binder" chain was noised. Additionally, and in contrast to the original RFdiffusion model trained for protein binder design, up to 50% of the noised monomer structure had sequence provided in the noised region. For hetero-complexes, up to 50% of the target chain backbone was also noised, while its sequence was provided to RFdiffusion. This permits RFdiffusion to condition on the sequence of the target chain in the absence of three-dimensional structure.

To permit specification of the secondary structure of the target (when three-dimensional coordinates are not provided), secondary structure and "block adjacency" [14] information were

provided to RFdiffusion in exactly the manner described in Watson et al[14]. Briefly, 50% of the time, RFdiffusion was provided with a (partially masked; 0-75%) secondary structure of the example protein chain/hetero-complex, and (an independently-sampled) 50% of the time a (partially masked; 0-75%) "block adjacency" of the protein chain/hetero-complex. Additionally, 50% of the time, the whole inter-chain "block adjacency" was masked in hetero-complex examples. This permits RFdiffusion to condition on a (partially) pre-specified secondary structure (and/or adjacency information) of the target peptide. This version of RFdiffusion was trained for seven epochs.

To design binders using RFdiffusion through secondary structure specification, foreach target, approximately ten thousand diffused designs were generated through sequence input of the target with the additional secondary structure specification. The resulting library of backbones were sequence designed using ProteinMPNN[21], followed by AF2+initial guess[23]. The resulting designs were filtered in the same way as the designs from the aforementioned sequence input diffusion process.

Backbone extension for VP48 binder design

During the design campaign, it was noticed not all designs provided sufficient interactions to the whole sequence of the target, especially the loopy regions. To explore and guide RFdiffusion to make more interactions around certain regions, we selected 20 AF2 passing designed complexes from the round one design campaign, based on the above criteria and manual selection. For each base design, we requested RFdiffusion to extend the binder backbone with 10-20 amino acids from either N terminal, or C terminal, or both (depending on where the loopy region was located. This was done with the inpaint flavor published in the original RFdiffusion work[14]. 2,000 trajectories were performed each run, followed by the same MPNN and AF2 predictions as above.

Computational filtering

Precise metrics cutoffs changed for each design campaign to get to an orderable set, but largely focused on interface pAE <10, pLDDT >90, number of hydrogen bonds >11, RMSD < 0.5, sap score <45 and Rosetta ddG < -40[44] .

Gene construction of peptide binders

The designed protein sequences were optimized for expression in *E. coli*. Linear DNA fragments (eBlocks, Integrated DNA Technologies) encoding design sequences included overhangs suitable for Golden Gate cloning into LM670 vector (Addgene #191552) for protein expression in *E.coli*. LM670 is a modified expression vector containing a Kanamycin resistance gene, a ccdB lethal gene between BsaI cut sites, and a C-terminal hexahistidine, commonly referred to as His tag.

Binding screening by Bio-layer interferometry (BLI) or co-lysis of binder and target peptide

For screening for all designs except the ones of partial diffusion design for Amylin-68n(Fig.2a), the designs were screened by BLI (method details described in below relative description). Linear gene fragments encoding binder design sequences were cloned into LM670 using Golden Gate assembly.Golden Gate subcloning reactions of peptide binders were constructed in 96-well PCR plates in 4μL volume. 1μL reaction mixtures were then transformed into a chemically competent expression strain (BL21 (DE3)). After 1 hour recovery in 100 μL SOC medium, the transformed cell suspensions were directly transferred into a 96-deep well plate containing 900 μL of LB media with Kanamycin. After overnight incubation in 37 ºC, 100 μL of growth culture were inoculated into 96-deep well plates containing 900 μL of auto-induction media (autoclaved TBII media supplemented with Kanamycin, 2mM MgSO4, 1X 5052). After overnight incubation (6 hours at 37 ºC followed by additional 18 hours at 30ºC), cells were harvested by centrifugation (15 min at 4000 x g). Bacteria were lysed for 15 minutes in 200 μL lysis buffer (1x BugBuster (Millipore#70921-4), 0.01 mg/mL DNAse, 1 tablet of pierce protease inhibitor tablet/50 mL culture). Lysates were clarified by centrifugation at 4000 g for 10 minutes, before purification on Ni-charged MagBeads (genscript #L00295; wash buffer: 25 mM Tris pH 8.0, 300 mM NaCl, 30 mM Imidazole; elution buffer: 25 mM Tris pH 8.0, 300 mM NaCl, 400 mM Imidazole). Subsequently, the elutions were directly subjected to a BLI test and the final concentration is approximately 1 μM. The designs exhibiting binding signals were subsequently analyzed by BLI through titration.

For Amylin-68n, the designs from partial diffusion were expressed and purified using the same way as mentioned above. In addition to the designs, plasmids expressing target peptide fused with

sfGFP (no His tag) were transformed into BL21 (DE3) cells, and overnight outgrowths were cultured in 5 mL of LB media with Kanamycin. After overnight incubation in 37 ºC and 250 rpm, growth cultures were inoculated into 50 mL auto-induction media. After overnight incubation in 37 ºC and 250 rpm, cells were harvested by centrifugation (15 min at 4000 x g), then resuspended in 20 mL lysis buffer (25 mM Tris-HCl, 150 mM NaCl, 0.1 mg/mL lysozyme, 10 µg/mL DNAse I, 1 mM PMSF). 100 µL of lysate of each binder were mixed with 100 µL of lysate of target peptide fused with sfGFP and incubated at room temperature for 15 min for co-lysis and target binding to the binders. Mixed lysates were applied directly to a 100 µL bed of Ni-NTA agarose resin in a 96-well fritted plate equilibrated with a Tris wash buffer. After sample application and flow through, the resin was thoroughly washed, and samples were eluted in 200 µL of a Tris elution buffer containing 300 mM imidazole. All eluates were sterile filtered with a 96-well 0.22µm filter plate (Agilent 203940-100) prior to size exclusion chromatography. Protein binders were then analyzed for target binding via sfGFP co-elution with the His-tagged binder. High-performance liquid chromatography (HPLC) analyses were conducted using an Agilent HPLC system (<product name>). Co-lysates were run on a Superdex200 Increase 5/150 GL column (Cytiva 28990945) with buffer of 25 mM Tris-HCl, 150 mM NaCl. To assess the binding interaction between the target and the binder, we monitored the elution profile of sfGFP using an absorbance wavelength of 395 nm, alongside a simultaneous measurement at 280 nm for total protein content to determine the extent of overlap between 395 nm and 280 nm, which indicates the binding interaction.

Medium scale protein expression and purification *E.coli* for hits from screening

For further validation, the initial hits were expressed at 50 mL scale via autoinduction for approximately 24 hours, in which the first 6 hours cultures were grown at 37 ºC and the remaining time at 22 ºC. Cultures were harvested at 4000 g for 10 minutes and resuspended in approximately 20 mL lysis buffer (25 mM Tris-HCl, 150 mM NaCl, 0.1 mg/mL lysozyme, 0.01 mg/mL DNAse, 1 mM PMSF,1 tablet of pierce protease inhibitor tablet/50 mL culture). Sonication was performed with a 4-prong head for 5 minutes total, 10 s pulse on-off at 80% amplitude. The resulting lysate was clarified by centrifugation at 14000 g for 30 minutes. Lysate supernatants were applied directly to a 1 mL bed of Ni-NTA agarose resin equilibrated. After sample application and flow through, the resin was thoroughly washed, and samples were eluted by an elution buffer containing 400 mM imidazole. After elution, protein samples were filtered and injected into an autosampler-

equipped Akta pure system on a Superdex S75 Increase 10/300 GL column at room temperature. The SEC running buffer was 25mM Tris-HCl, 150mM NaCl pH 8. Protein concentrations were determined by absorbance at 280 nm using a NanoDrop spectrophotometer (Thermo Scientific) using their extinction coefficients and molecular weights obtained from their amino acid sequences.

Bio-layer interferometry (BLI) binding experiments

BLI experiments were performed on an Octet Red96 (ForteBio) instrument, with streptavidin coated tips (Sartorius Item no. 18-5019). Buffer comprised 1X HBS-EP+ buffer (Cytiva BR100669) supplemented with 0.1% w/v bovine serum albumin. Prior to target loading, each design was tested for binding against unloaded tips. 50 nM of biotinylated target protein was loaded on the tips for 50 s followed by a 60 s baseline measurement. After loading, all designs underwent a 60 s baseline, 300 s association and 200 s dissociation. Baseline measurements of unloaded tips were subtracted from their matched measurement of the loaded tip. The hits were taken forward for further titration experiments where concentration, association and dissociation times were chosen based on apparent affinity from the single point screen. Global kinetic fitting was used to determine KDs across the dilution series.

Circular dichroism (CD) experiments

For CD experiments, designs were diluted to 0.4mg/ml in 25 mM Tris-HCl and 150 mM NaCl. Spectra were acquired on a JASCO J-1500 CD Spectrophotometer. Thermal melt analyses were performed between 25 ^{o}C and 95 ^{o}C, measuring CD at 222 nm. All reported measurements were acquired within the linear range of the instrument.

Affinity enrichment of Amylin analyzed by LC-MS/MS

Bead preparation

Anti-amylin binder-coated beads were prepared by conjugating each amylin-targeted binder (Amylin-68n) to paramagnetic M280 Tosylactivated beads (Invitrogen, MA, USA). Each sample reaction conjugated 1 µg of binder to 225 µg of beads. Beads were blocked with a solution of 0.01% bovine serum albumin (BSA) in 0.2 M Tris to minimize non-specific interactions. An off-target binder-conjugated bead was included for quantification of non-specific binding. A BSA-blocked

bead without a bound binder was used as a negative control and an anti-GPVGPSGPPGK (GPVG) peptide monoclonal antibody-conjugated bead was used as a positive control for the affinity binding step.

Sample preparation

Human amylin peptide (non-amidated) was purchased from Anaspec (Fremont, CA, USA) and reconstituted to 2 mg/mL in dimethylsulfoxide (DMSO). A secondary peptide stock (diluted into 50 µM in 5% acetonitrile, 0.1% formic acid, 0.01% BSA in water) was reduced with dithiothreitol (10 mM final concentration) and alkylated with iodoacetamide (30 mM final concentration). Excess iodoacetamide was quenched with additional dithiothreitol (5 mM final added concentration). This solution was diluted to a working stock of 10 µM with dilution solvent. Aliquots of the working stock were made in 1.5 mL LoBind tubes and stored at -20°C to avoid repeated freeze/thaw cycles.

Human specimens

Human plasma samples were composed of pooled de-identified leftover clinical samples obtained from the clinical laboratories at the University of Washington Medical Center. The use of de-identified leftover clinical samples was reviewed by the University of Washington Human Subjects Division (STUDY00013706).

Affinity enrichment

Amylin capture experiments were performed using three types of coupled beads (Amlin-68n, off-target binder, BSA-blocked) in phosphate-buffered saline (PBS) containing 0.1% 3-((3-cholamidopropyl) dimethylammonio)-1-propanesulfonate (CHAPS) as well as pooled normal human EDTA-anticoagulated plasma.

Samples were prepared by spiking the working stock of alkylated amylin to a final concentration of 20 nM in 100 µL of either PBS-CHAPS or pooled plasma. Additional PBS-CHAPS was added to each sample, followed by coupled beads. GPVG peptide and anti-GPVG monoclonal antibody-conjugated beads were added to each sample as a positive control. The mixtures were shaken for 1 hr at 900 rpm and room temperature (Thermomixer, Eppendorf, Framingham MA). The

supernatant was removed and the beads were washed twice with 200 µL of PBS-CHAPS. Bound peptides were eluted in 50 µL of elution solvent (20% acetic acid, 10% acetonitrile, 10% DMSO, 0.001% BSA in water) with shaking for 8 min (900 rpm, room temperature). Each bead type (two anti-amylin binders, one off-target binder, one BSA-blocked) was assessed in separate samples and each was prepared in triplicate.

Sample analysis was performed by liquid chromatography-tandem mass spectrometry using a Shimadzu Nexera LC-XR HPLC (Columbia, MD, USA) coupled to a Sciex 6500+ triple quadrupole tandem mass spectrometer (Framingham, MA, USA) in multiple reaction monitoring (MRM) mode. Specifications for the liquid chromatography, mass spectrometer, and MRM methods are included in Supplementary Tables x, x, and x.

Data analysis

Data processing was performed with Skyline Daily (version 23.1.1.459). Chromatographic peak area was calculated by summing the peak area of all transitions for each peptide. The chromatographic peak areas observed during blank (elution solvent) injections were subtracted as background from sample peak areas before performing further data reduction. Signal from BSA and GPVG beads were for quality control of the assay and evaluated prior to processing of the experimental data.

Seven types of samples were analyzed:

1. Group A: Alkylated amylin peptide spiked directly into elution solvent served as the reference peak area for 100% recovery of amylin peptide.

2. Group B: Paramagnetic tosyl-activated beads conjugated to an off-target binder were incubated in PBS-CHAPS spiked with alkylated amylin. The peak area of this negative control was used to quantify nonspecific binding.

3. Group C: Amylin-targeted binders conjugated to paramagnetic tosyl-activated beads were incubated in PBS-CHAPS spiked with alkylated amylin. The peak areas of these samples were used to quantify the percent recovery of amylin by affinity enrichment.

4. Group D: An off-target binder conjugated to paramagnetic tosyl-activated beads was incubated with unspiked plasma. The peak area of this negative control was used to quantify the nonspecific signal from beads binding to plasma components.

5. Group E: Amylin-targeted binders conjugated to paramagnetic tosyl-activated beads were incubated with unspiked plasma. The peak areas observed in these samples were used to quantify the nonspecific signal from the binders binding to plasma components (i.e., assuming no non-amidated amylin in normal plasma).

6. Group F: An off-target binder conjugated to paramagnetic tosyl-activated beads was incubated with spiked plasma. The peak area of this negative control was used to quantify nonspecific binding.

7. Group G: Amylin-targeted binders conjugated to paramagnetic tosyl-activated beads were incubated with spiked plasma. The peak areas of these samples were used to quantify percent recovery of amylin by affinity enrichment.

The percent recovery of each binder-coated bead type was calculated using the following equations:

$$Percent\ recovery_{buffer} = \frac{Group\ C - Group\ B}{Group\ A}$$

$$Percent\ recovery_{Plasma} = \frac{(Group\ G - Group\ F) - (Group\ E - Group\ D)}{Group\ A}$$

Supplementary Table 2. Amylin transitions monitored

Peptide Sequence	Q1 (m/z) (charge state)	Q3 (m/z)	Ion type
KCNTATCATQRLANFLVHSSNNFGAILSSTNVGSNTY	976.90 (4+)	921.59	b_{26}^{3+}
		988.48	b_{28}^{3+}
		931.90	b_{36}^{3+}
		541.18	y_5^{+}
GPVGPSGPPGK	475.26 (2+)	795.44	y_9^{+}
		696.37	y_8^{+}

		639.35	y_7^+
		398.24	y_4^+
		301.19	y_3^+
		155.08	b_2^+
GPVGPSGPPGK[$^{13}C_6$, $^{15}N_2$]^ K^ = $^{13}C_6H14^{15}N_2O2$ (+8 Da)	479.27 (2+)	704.38	y_8^+
		647.36	y_7^+
		406.25	y_4^+

Supplementary Table3. Liquid chromatography parameters		
Mobile phase	Phase A: 0.2% formic acid in water	
	Phase B: 0.2% formic acid in acetonitrile	
Column	Acquity UPLC HSS T3 1.8µm (C18, 2.1x50 mm, pore size 100 Å) (Waters, Milford, MA, P/N 186003539)	
Temperature	45°C	
Flow rate	0.3 mL/min	
Injection volume	10µL	
Gradient	0-0.5 min	20% B at 0.3 mL/min
	7.5 min	60% B at 0.3 mL/min
	9.5 min	98% B at 0.3 mL/min
	11.0 min	98% B at 0.3 mL/min
	11.1 min	20% B at 0.3 mL/min
	12.5 min	20% B at 0.3 mL/min

Supplementary Table 4. Mass spectrometry parameters	
Source Polarity	ESI+
Curtain Gas	35
Collision Gas	9
Ionspray Voltage	5500 V
Source Temperature	400°C
Ion Source Gas 1	40

Ion Source Gas 2	40

Preparation of SSM libraries

We performed SSM studies for some of the designed peptide–protein binding pairs to gain a better understanding of the peptide-binding modes, and to search for improved peptide binders. For CP35, we ordered a SSM library covering all the 159 amino acids. The chip synthesized DNA oligos for the SSM library were then amplified and transformed to EBY100 yeast together with a linearized pETCON3 vector. Each SSM library was subjected to an expression sort first, in which the low-quality sequences due to chip synthesizing defects or recombination errors were filtered out. The collected yeast population, which successfully expresses the designed mutants, will be regrown, and subjected to the next round of peptide-binding sorts. Two rounds of with-avidity sorts were applied at 1 μM concentration of C-peptides followed by 1 rounds of without-avidity sorts with C-peptide concentrations at 200nM, 40 nM, 8nM, 1.6nM and 0.32nM. The peptide-bound yeast populations were collected and sequenced using the Illumina NextSeq kit. The mutants were identified and compared to the mutants in the expression libraries. Enrichment analysis was used to identify beneficial mutants and provide information for interpreting the peptide-binding modes. For each mutant, the fraction of cells collected in each of 5 titration sorts of decreasing concentration is measured. The SortingConcentration50 (SC50), the concentration where 50% of the expressing cells are collected, is calculated and plotted in heat maps for the SSM analysis.

X-ray crystallography

Crystallization experiments were conducted using the sitting drop vapor diffusion method. Initial crystallization trials were set up in 200 nL drops using the 96-well plate format at 20 ˚C. Crystallization plates were set up using a Mosquito LCP from SPT Labtech, then imaged using UVEX microscopes and UVEX PS-256 from JAN Scientific. Diffraction quality crystals formed in 0.1M succinic acid, sodium phosphate monobasic monohydrate, glycine mixture at pH 6 and 30% w/v PEG 1000 for Amylin-22. For g3bp1-11 diffraction quality crystals appeared in 0.05 M Calcium chloride dihydrate, 0.1 M BIS-TRIS pH 6.5, and 30% v/v Polyethylene glycol monomethyl ether 550.

Diffraction data was collected at the National Synchrotron Light Source II on beamline 17-ID-1 (AMF) for Amylin-22$_{\alpha\beta L}$ and Advanced Light Source beamline 821 for g3bp1-11. X-ray intensities and data reduction were evaluated and integrated using XDS[45] and merged/scaled using Pointless/Aimless in the CCP4 program suite[46]. Structure determination and refinement starting phases were obtained by molecular replacement using Phaser[47] using the designed model for the structures. Following molecular replacement, the models were improved using phenix.autobuild; with rebuild-in-place to false, and using simulated annealing. Structures were refined in Phenix[48]. Model building was performed using COOT[49]. The final model was evaluated using MolProbity[50]. Data collection and refinement statistics are recorded in Table 5. Data deposition, atomic coordinates, and structure factors reported in this paper have been deposited in the Protein Data Bank (PDB), http://www.rcsb.org/ with accession code 9CC5 and 9CC6.

Supplementary table 5. Data collection and refinement statistics.

	Amylin-22$_{\alpha\beta L}$ (PDB Code: 9CC5)	G3bp1-11 (PDB Code: 9CC6)
Resolution range	33.32 - 1.87 (1.94 - 1.87)	31.43 - 2.4 (2.48 - 2.4)
Space group	*P 2$_1$ 2$_1$ 2$_1$*	*P 2$_1$*
Unit cell	33.33, 34.51, 127.68; 90, 90, 90	38.43, 42.39, 40.63; 90, 105.53, 90
Unique reflections	12855 (1372)	4698 (410)
Multiplicity	6.6 (6.8)	5.3 (5.0)
Completeness (%)	99.38 (99.28)	93.38 (92.0)
Mean I/sigma(I)	7.94 (1.22)	11.0 (2.2)
Wilson B-factor	28.60	38.45
R-merge	0.1598 (1.79)	0.033 (0.623)
R-pim	0.06738 (0.7403)	0.032 (0.152)
CC$_{1/2}$	0.999 (0.769)	0.993 (0.956)

Reflections used in refinement	12756 (1372)	4697 (410)
R-work	0.2256 (0.2949)	0.2199 (0.2709)
R-free	0.2721 (0.3400)	0.2567 (0.2856)
Number of non-hydrogen atoms	1335	1197
macromolecules	1289	1190
solvent	46	7
Protein residues	163	150
RMS(bonds)	0.015	0.003
RMS(angles)	1.31	0.60
Ramachandran favored (%)	95.60	98.63
Ramachandran allowed (%)	4.40	1.37
Ramachandran outliers (%)	0.00	0.00
Average B-factor	35	46
macromolecules	35	46
solvent	40	43

The highest-resolution shell is shown in parentheses.

Cell culture

HeLa cells were cultured in DMEM (Gibco, 11965-092) at 37 °C in a humidified atmosphere containing 5% CO2, supplemented with 10% (v/v) FetalClone II serum (Cytiva, SH3006603) and 1% penicillin–streptomycin (ThermoFisher, 15140122).

Generation of IL2RG-knockout HeLa cells by CRISPR–Cas9 gene targeting

Pooled IL2RG-knockout HeLa cells was generated using the Gene Knockout kit V2 from Synthego, using multi-guide sgRNA targeting IL2RG (guide 1: CAUACCAAUAAUGCAGAGUG, guide 2: UCGAGUACAUGAAUUGCACU and guide 3: GAAACACUGAGGGAGUCAGU). The ribonucleoprotein complex with a ratio of 4.5:1 of sgRNA and Cas9 was delivered following the protocol of the SE Cell Line 4D-Nucleofector™ X Kit S (Lonza, V4XC-1032), using the nucleofection program CN-114 on the Lonza 4D X unit.

Transient transfection

Plasmids for IL2RG-30-mScarlet, IL2RG-EGFP were synthesized and cloned by Genscript USA, Inc. HeLa cells were seeded at 70–80% confluency in a chambered coverslip with 18 wells (ibidi, 81816). At the same time, HeLa cells were reverse-transfected using Lipofectamine 3000 transfection reagent (ThermoFisher, L3000008) according to the manufacturer's protocol.

Fluorescence imaging using 3D structured illumination microscopy

4-color, 3D images were acquired with a commercial OMX-SR system (GE Healthcare). Toptica diode lasers with excitation at 488 nm, and 568 nm were used. Emission was collected on three separate PCO.edge sCMOS cameras using an Olympus 60× 1.42NA PlanApochromat oil immersion lens. 512×512 images (pixel size 6.5 μm) were captured with no binning. Acquisition was controlled with AcquireSR Acquisition control software. Z-stacks were collected with a step size of 250 nm. Images were deconvolved in SoftWoRx 7.0.0 (GE Healthcare) using the ratio method and 200 nm noise filtering. Images from different color channels were registered in SoftWoRx using parameters generated from a gold grid registration slide (GE Healthcare).

Thioflavin-T (ThT) fluorescence assay

Amylin fibrils at various growth stages (0 h, 3 h and 24 h) were adequately mixed with ThT at molar ratio 1:1 and added into 96-well-plates containing different types and concentrations of binders (Am75, Am36, Am22, Am68n). The samples were then incubated at 37 °C for 1-18 hours with 600 rpm orbital shaking. ThT fluorescence signals were measured using a Thermo Varioskan Flash Multi Detection Microplate Reader (0 h and 3 h) or a Perkin elmer EnSight Multifunctional

Microplate Reader (24 h） with excitation wavelength at 440 nm and an emission wavelength at 482 nm.

Negative-stain electron microscopy (NS-EM) experiment

Samples for negative-stain electron microscopy were dropped onto freshly glow-discharged carbon-coated copper grids and incubated for 1 minute, and excess sample was removed by blotting on filter paper. The grids were then stained with 2 % (w/v) uranyl acetate for 1 minute, and excess uranyl acetate was blotted off. Finally, the grids were examined using a Tecnai Spirit transmission electron microscope (FEI) at an acceleration voltage of 120 kV.